Convective Modes for Significant Severe Thunderstorms in the Contiguous United States. Part III: Tropical Cyclone Tornadoes

ROGER EDWARDS, ANDREW R. DEAN, RICHARD L. THOMPSON, AND BRYAN T. SMITH

NWS Storm Prediction Center, Norman, Oklahoma

(Manuscript received 23 September 2011, in final form 20 June 2012)

ABSTRACT

A gridded, hourly, three-dimensional environmental mesoanalysis database at the Storm Prediction Center (SPC), based on objectively analyzed surface observations blended with the Rapid Update Cycle (RUC) model-analysis fields and described in Parts I and II of this series, is applied to a 2003–11 subset of the SPC tropical cyclone (TC) tornado records. Distributions of environmental convective parameters, derived from SPC hourly mesoanalysis fields that have been related to supercells and tornadoes in the midlatitudes, are evaluated for their pertinence to TC tornado occurrence. The main factor differentiating TC from non-TC tornado environments is much greater deep-tropospheric moisture, associated with reduced lapse rates, lower CAPE, and smaller and more compressed distributions of parameters derived from CAPE and vertical shear. For weak and strong TC tornado categories (EF0–EF1 and EF2–EF3 on the enhanced Fujita scale, respectively), little distinction is evident across most parameters. Radar reflectivity and velocity data also are examined for the same subset of TC tornadoes, in order to determine parent convective modes (e.g., discrete, linear, clustered, supercellular vs nonsupercellular), and the association of those modes with several mesoanalysis parameters. Supercellular TC tornadoes are accompanied by somewhat greater vertical shear than those occurring from other modes. Tornadoes accompanying nonsupercellular radar echoes tend to occur closer to the TC center, where CAPE and shear tend to weaken relative to the outer TC envelope, though there is considerable overlap of their respective radial distributions and environmental parameter spaces.

1. Introduction and background

A rather broad body of literature has accumulated in the realm of tropical cyclone (TC) tornado research over the past several decades, dealing primarily with climatology and distribution (e.g., Novlan and Gray 1974; Schultz and Cecil 2009), but also covering notable individual cases (e.g., Orton 1970; McCaul 1987) and sounding-based observational assessments (e.g., McCaul 1991; Curtis 2004). More recently, applied research has expanded the TC tornado knowledge base into realms such as numerical modeling (e.g., McCaul and Weisman 1996; Morin et al. 2010) and Doppler radar examinations of tornadic storms (e.g., Spratt et al. 1997; McCaul et al. 2004; Rao et al. 2005). Agee and Hendricks (2011) associated the presence of Doppler radar with a large increase in TC tornado reports specific to Florida (i.e., pre-Doppler era tornadoes were ''severely underestimated'' in that state). For an expansive review of the evolution of TC tornado-related research and forecasting, see Edwards (2012).

The fundamental conceptual and physical tenets of midlatitude supercell forecasting, in an ingredients-based framework (e.g., McNulty 1978; McNulty 1985; Doswell 1987), are valid for TC supercells; however, systematic differences in the relative magnitudes of moisture, instability, lift, and shear in TCs (e.g., McCaul 1991) contribute strongly to the challenge of forecasting tornadoes in that setting. Such differences may be related to meso- and smaller-scale boundaries within the TC envelope—whether antecedent or developing in situ—that can influence convective character and tornado potential (e.g., Fig. 3 in McCaul et al. 2004; Edwards and Pietrycha 2006). There also is a growing realization that some TC tornadoes are not necessarily supercellular in origin, as shown in our results below. The challenge of TC tornado prediction remains hampered by incomplete insight into supportive environmental influences from the

Corresponding author address: Roger Edwards, NWS Storm Prediction Center, Ste. 2300, 120 Boren Blvd., Norman, OK 73072. E-mail: roger.edwards@noaa.gov

DOI: 10.1175/WAF-D-11-00117.1

cyclone (meso α to meso β) and convective (at 10s of km and smaller) scales.

Hypothetically, the separation of tornadic convective elements (supercellular or not) from surrounding convection—in other words, discrete storms versus those embedded in clusters or bands—favors the potential for more numerous and/or more damaging tornadoes. Testing this idea was one of the motivators for the determination of convective modes herein. Idealized numerical simulations (McCaul and Weisman 1996) have indicated that, because of the large moisture content and related lack of robust evaporative cooling in low levels, discrete supercells in TCs should have weak cold pools. Although McCaul and Weisman suggested this as a potential factor in the weakness of TC tornadoes in general, compared to their counterparts in midlatitude systems, those simulations did not account for either kinematic or baroclinic inhomogeneities, such as those accompanying spiral convergence bands or zones of differential diabatic heating. Observationally, storm-scale baroclinicity has been measured within TCs, such as equivalent potential temperature (θ_e) deficits of up to 12 K beneath spiral bands over water documented by Barnes et al. (1983). Furthermore, from an analysis of buoy data, Cione et al. (2000) showed thermal deficits accompanying vigorous convective bands, as well as a decrease in air–sea thermal deficit inward with respect to the dense precipitation of the inner region of hurricanes. The latter is consistent with the inward weakening of buoyancy climatologically documented by McCaul (1991).

Given the relative coarseness of surface observations over water, and over some land areas, such meso-β to convective-scale processes may not be readily apparent to the operational forecaster and, instead, may be inferred by indirect evidence such as convective mode and persistence. Those, in turn, can be influenced by merging and clustering of storms and precipitation areas common to the dense precipitation regimes of TCs. Barnes et al. (1983) also documented a lack of discrete storms with inward extent toward the TC center, which may be related to the merging regime and/or the relatively weak CAPE in the TC core region. The presence of an objectively analyzed environmental dataset at SPC (Schneider and Dean 2008) that included numerous landfalling TC situations, and the ability to classify storm modes, permits these issues to be investigated holistically in the TC setting.

As with midlatitude convective phenomena of similar spatial scales, there remain caveats about the utility of the automated analyses in the TC setting. The accuracy of the analyses is uncertain at scales $<$40 km, which covers TC supercells, most nonsupercellular tornadic echoes found in this study, and the short axes of spiral bands. Further, the Rapid Update Cycle (RUC) model basis[1] for the analyses was not constructed to resolve either hurricane winds or related extreme pressure gradients, nor the wind transitions from ocean to land in a hurricane. These factors become less important away from extreme gradients—in the outer parts of hurricanes where most of their tornadoes occur—and in TCs weaker than hurricane intensity at tornado time, which account for most events herein.

Companion studies determine radar-based convective modes with nontropical severe thunderstorms producing damaging thunderstorm winds, large hail, and tornadoes (Smith et al. 2012, hereafter Part I), then focus on the near-storm environments of tornadic midlatitude supercells and tornadic quasi-linear convective systems (Thompson et al. 2012, hereafter Part II). This third part of this study similarly presents some findings for the storm modes and near-convective environments, as applied specifically to TC tornado events that occurred during the period 2003–11. For clarity, ''storm'' hereafter will refer to those convective elements, on horizontal scales of 10^0–10^1 km, specifically responsible for tornadoes. This term is used instead of ''cell'' since (as shown herein) some tornadic storm modes are not unambiguously or discretely cellular. The acronym ''TC'' will be used to refer to the tropical cyclone as a whole.

2. Data and methods

TC tornado data come from the 1995–2011 ''TCTOR'' database (Edwards 2010) at SPC. The three most prolific TC tornado seasons in the TCTOR dataset—2004, 2005, and 2008—fall within the subset analyzed in this study, except for the missing effective-layer-based 2004 environmental data, as detailed in section 3d.

The number of *tornado events* examined here (730) is different than the number of actual tornadoes contained in the 2003–11 temporal subset of TCTOR (826), for the following reasons: 1) segmenting by county of the tornado data in Parts I–III, whereas TCTOR is whole-tornado data, and 2) the spatiotemporal gridding and filtering technique detailed in Part I, which distills proximal tornado reports to single grid events. For this purpose, a tornado event (hereafter ''tornado'') constitutes the county segment of a tornado report that was

[1] The Rapid Refresh model (Benjamin et al. 2007) operationally replaced the RUC on 1 May 2012. Its efficacy in the TC environment, both on its own and as an influence in SPC mesoanalyses, is yet to be determined.

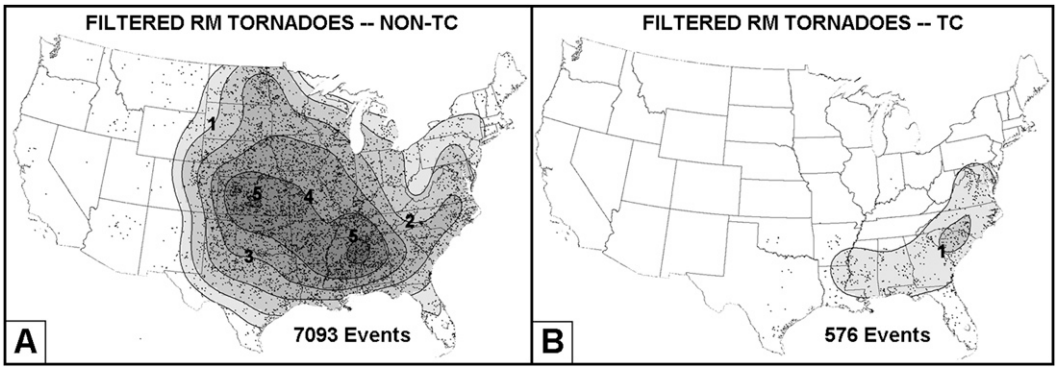

FIG. 1. Kernel density estimate on a 40 km × 40 km grid of filtered, continental U.S. tornado events in right-moving (RM) supercell modes: (a) non-TC in origin and (b) from TCs only. Sample sizes are given for each. Minimum contour is 0.5 events per 10 yr estimate based on 2003–11 data. Labeled contours begin at 1 event per 10 yr. Black dots represent events that formed the basis of the kernel density estimate, and the progressively darker gray fill represents a higher event estimate.

assigned the maximum rating on the enhanced Fujita (EF) scale[2] rating in each 40-km grid square, for the analysis hour containing the report (e.g., a 2055 UTC tornado is assigned a 2000 UTC environment). These spatial and temporal bounds were chosen for comparison and analyses of environmental parameters with convective modes associated specifically with TC tornadoes, similar to analyses performed for a larger, non-TC dataset of tornadic and nontornadic significant severe storm environments in Part II. Figures 1 and 2 depict the geographic distribution and spatial density of the filtered tornadoes involved herein.

The environmental-analysis time frame began in 2003, using the same database as described by Schneider and Dean (2008). To summarize, an objectively analyzed field of surface observations, using the hourly RUC (after Benjamin et al. 2004) analysis as a first guess, is combined with 40-km gridded RUC model data aloft in an identical manner to that used in creating the SPC hourly mesoscale analyses (Bothwell et al. 2002). This provides hourly, three-dimensional fields from which numerous parameters can be derived that are commonly used for sounding analysis of the moist-convective environment.

Volumetric radar data for this era were interrogated as described in Part I, in order to assign a convective mode to each tornadic event. Mode designation was necessarily subjective, but followed specific guidelines. Ten tornadic storm modes appeared in TCs, assigned according to the same archetypical guidelines established in Part I. Radar-based classifications are summarized here with the name and sample size of each event in italics (percentages sum to 101 because of rounding):

- *discrete right-moving supercell (RM)*—storms accompanied by deep, persistent mesocyclones[3] generally characterized by ≥20 kt (10 m s^{-1}) rotational velocity at most ranges, and distinct from surrounding echoes at ≥35 dB*Z*; *249 events (34%)*;[4]
- *quasi-linear convective system (QLCS)*—contains contiguous reflectivities >35 dB*Z* for a length ≥100 km at ≥3/1 aspect ratio; nonsupercellular; includes storms embedded in lines; *21 events (3%)*;
- *cluster*—as with QLCS, but with an aspect ratio <3/1; nonsupercellular; included disorganized and/or amorphous reflectivity patterns; *25 events (3%)*;
- *supercell in line*—meets velocity and continuity guidelines for supercells but is embedded in a QLCS; *70 events (10%)*;
- *supercell in cluster*—meets velocity and continuity guidelines for supercells but is embedded in a cluster; *257 events (35%)*;[5]
- *discrete nonsupercell*—lacks horizontal rotation, or rotational characteristics are too weak and transient to classify even as ''marginal'' (below); *13 events (2%)*;

[2] The term ''EF'' is used for the damage ratings of all tornadoes herein, including those rated prior to the enhanced Fujita scale's implementation in February 2007, because of the correspondence in F- and EF-scale ratings intrinsic to the development of the latter (WSEC 2006).

[3] Left-moving (anticyclonic) supercells, a category used for midlatitude events in Part I and Part II, did not appear in our TC examinations.

[4] Due to data outage, one event from this subset had no environment data except STP.

[5] Due to a data outage, one event from this subset had no environment data except STP; two others lacked all but SCP and STP.

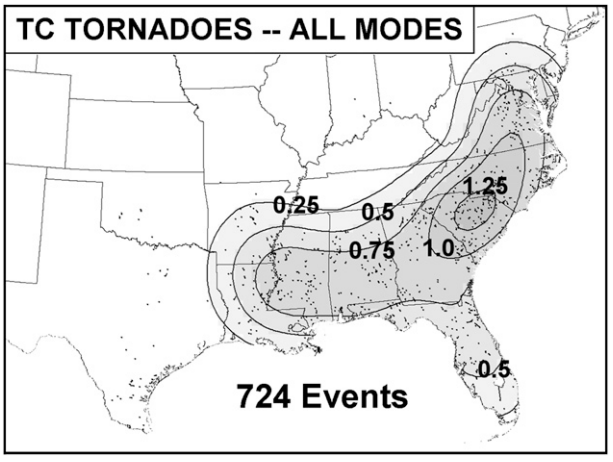

FIG. 2. As in Fig. 1b, but for all convective modes. Minimum contour is 0.25 events per 10 yr, based on 2003–11 data. Labeled contour intervals are 0.25 events per 10 yr. Map is cropped to affected areas of the United States.

- *marginal discrete supercell*—shows at least brief, weak rotational characteristics but not fulfilling supercellular guidelines; *19 events (3%)*;[6]
- *marginal supercell in cluster; 37 events (5%)*;
- *marginal supercell in line; 7 events (1%)*;
- *cell in cluster, nonsupercellular; 26 events (4%)*; and
- *unclassified*—radar data missing or event out of range; *6 events (1%)*.

The three unambiguously supercellular categories (discrete, in line, in cluster) were analyzed separately and as a subgroup for this study. Within these supercellular categories, mesocyclones further were classified as weak, moderate, or strong, following a subjective three-bin ranking of range-dependent horizontal rotational velocity guidelines offered by Stumpf et al. (1998) and related nomograms (e.g., Andra 1997). A radar example of the discrete, tornadic TC supercell category is shown in Fig. 3. Partial or whole eyewalls associated with tornado reports[7] were classified as clusters.

Nonsupercell TC (NSTC) tornadoes likewise were examined in terms of their classified modes (e.g., clustered, linear, marginal supercell), distance from TC center (details in section 3), and as a second subgroup. Nonsupercell tornadoes have been studied formally for over two decades (e.g., Wakimoto and Wilson 1989), but not including those within TCs. Continuous spiral bands or segments of bands are treated as QLCSs if they meet the aforementioned mode criteria. Although tornadic bow echoes were a mode investigated in Part I, and have not been commonly documented in TCs that occurred during years prior to this study [e.g., the Florida ''Iron Bend'' storm described by Spratt et al. (1997)], no bow echoes were identified in association with TC tornadoes in the 2003–11 sample. It is unclear whether this is a function of limitations imposed on bulk sampling by the highly specialized nature of the environment studied, compared to the broader Part I sample that included midlatitude bow echoes, or of any actual physical tendency for TCs to produce a relative paucity of tornadic bows.

3. Analyses and findings

a. Error sources in tornado data

As with the national tornado database, close examination of TC tornado reports revealed a small number of apparent errors in time and/or location. By far, the primary source of such errors was the time of reports compared to radar signatures (or lack thereof). Where the location appeared accurate, but the apparently responsible echo (e.g., storm or mesocyclone) passed over the location earlier or later than the tornado report time, the time was adjusted to match the echo passage, as in Part I. This was done in 51 TC cases (7% of 730 total TC events), with an average absolute error of 44 min, and extremes of 2 and 210 min, not including one event that was +24 h off (wrong date entered in *Storm Data*). The most common time-error integer was 60 min, occurring in 16 cases; in other words, 31% of all documented time errors were displaced by precisely 1 h. Five of the 1-h absolute errors occurred in a county warning area straddling two time zones, indicating incorrect input of time zone; otherwise, the 1-h errors are suspected to arise from erroneous transposition of daylight with standard time in the process of local report logging. Sixteen of 51 (31%) of the *Storm Data* time errors were negative (i.e., the report occurred before the corresponding radar echo), including five of the 1-h errors. The average negative error was −63 min with extremes of −15 and −210. The average positive error (i.e., report lagged the radar echo) was 38 min with extremes of 2 and 107 min.

In a few instances, it was not immediately obvious which storm or echo, among multiple possibilities, was responsible for the report, and a guess had to be made based on echo timing and continuity. Three cases

[6] Because of a data outage, one event from this subset had no environmental information. Cases with most or partial missing environment data account for the presence of more total mode events than in the corresponding environmental analyses in section 3d and Fig. 7.

[7] See Edwards (2012) for further discussion on the uncertainties involving eyewall-tornado reports in general.

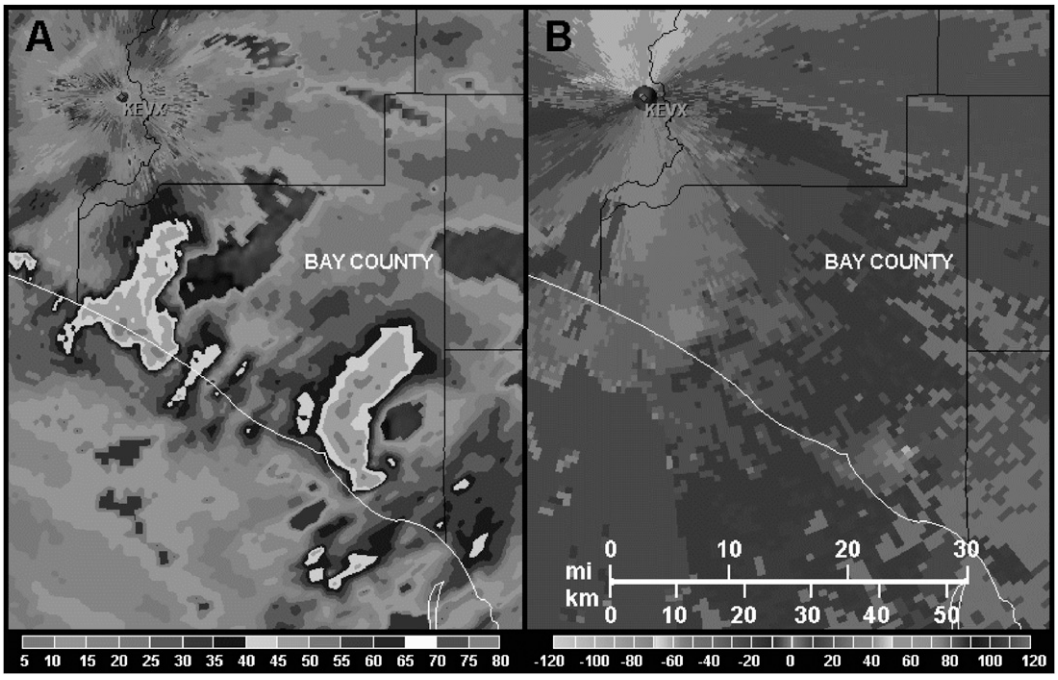

FIG. 3. Radar imagery at 0.5° beam tilt from Eglin Air Force Base (KEVX) WSR-88D at 0352 UTC 15 Sep 2004 of a discrete, tornadic supercell in southeastern Bay County, FL: (a) reflectivity, scale at bottom in dB*Z* and (b) storm-relative motion, scale at bottom in kt. Two associated, F1-rated tornadoes, 3 min apart, killed two people and injured eight others. North is up; mesocyclone was located ≈65 km southeast of KEVX (located in northwest quadrant of panels) at sampling time. This was storm A mapped in Fig. 1 of Baker et al. (2009).

required a change in a listing for report location (county and/or latitude–longitude entry) and two for date (both being time corrections across 0000 UTC). A few other cases had radar presentations so nebulous or otherwise uncertain that a time or place adjustment could not be made. Those time and/or location errors that were obvious and could be adjusted with confidence will be submitted for revision jointly in the nationwide SPC "ONETOR" and TCTOR databases (see Edwards 2010 for more details on that process). Other possible but not quantifiable sources for counting errors in TC situations include

- reports of tornadoes that actually were other phenomena, for example, gusts in gradient flow, wet microbursts, or damaging horizontal-shear vortices in the eyewall's inner rim (e.g., Fujita 1993) occurring without documented vertical continuity into its convective plume;
- tornadoes that were sufficiently weak and/or brief as to go unreported amid concurrent or subsequent hurricane conditions; and
- tornadoes that occurred in areas too remote to be witnessed or to cause noticeable damage and, as such, would go unreported.

The tornado ratings themselves also are subject to errors and uncertainties arising both from 1) the subjectivity and inconsistency inherent to the rating process (Doswell and Burgess 1988; Edwards 2003) and 2) damage obscuration by other TC effects. Hurricane-force winds in the inner portion of some TCs may augment or mask damage from tornadoes occurring in the same area, whether before, during, or after the passage of the TC core. Hydraulic damage (i.e., from storm surge, wave battering, or freshwater flooding) also may alter the effects of tornadoes. There is no known way to account consistently for these complications, other than to subjectively judge whatever damage-indicator documentation may be offered in text accompanying *Storm Data* event entries. No such information, in sufficient detail to cast doubt on an assigned rating, was available for events herein.

b. General results

Compared with non-TC tornadoes extracted from the Part I database, TCs heavily influenced the nationwide totals of tornadic supercells during the peak months of the North Atlantic hurricane season: August and September, with lesser relative contributions along the fringes in July and October (Fig. 4). Tornadic supercells

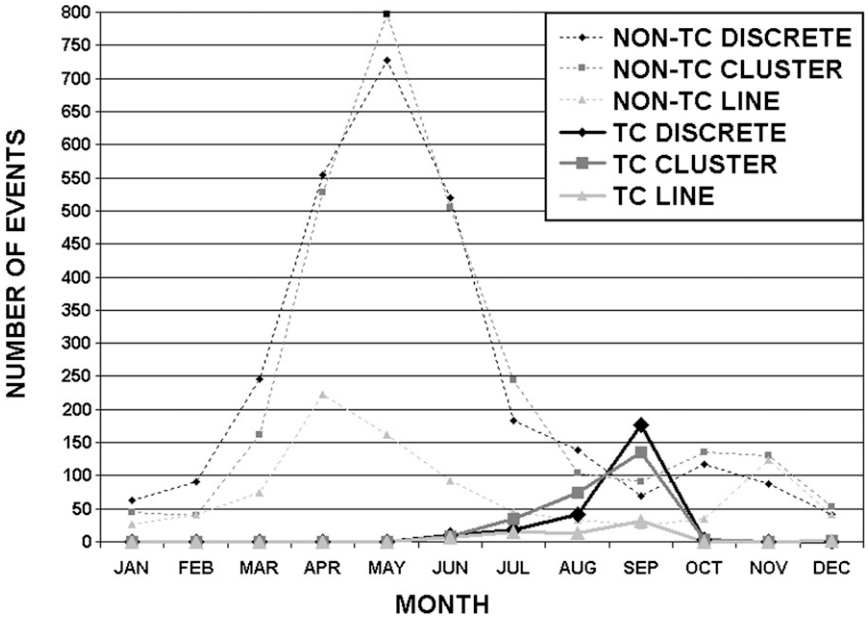

FIG. 4. Monthly graph of tornadic supercells, cumulatively for 2003–11, in three modes: discrete, embedded in a cluster, and embedded in a line. Dashed curves denote non-TC supercells (from Part I data); solid curves are TC events, per legend.

in TCs collectively accounted for 64% of all tornadic supercells in the conterminous United States during the month of September (2003–11), with the caveat that the two most prolific TC tornado seasons on record (2004 and 2005) are part of the analysis. During an otherwise subdued interval from late summer into early autumn, the predominant source of supercell tornadoes nationally was the TC. Overall, the grid-filtered number of TC tornado events in this 2003–11 dataset (730) was 7.3% of the number of grid-filtered non-TC tornado events (10 023; from the Part I database) or ≈6.8% of the nationwide tornado event total (10 753).

c. *Storm-mode analyses*

Discrete modes, whether supercellular or not, appeared more commonly outward from center, and as such, away from the central dense overcast and its underlying regions of relatively high-coverage, aggregated, and often complex reflectivity signatures. Of the storms responsible for TC tornadoes, 576 (79%) were unambiguously supercellular, 63 (9%) marginally supercellular, and the remaining 91 (12%) nonsupercellular. Among just the tornadic TC supercells, mesocyclone strength was classified as strong with 78 (14%), moderate with 134 (23%), and weak with 364 (63%). Thus, weak (strong) mesocyclones were far more (less) common with TC than non-TC events. The values for non-TC tornadic supercells from the Part I dataset were 3077 (43%) strong, 1855 (26%) moderate, and 3161 (30%) weak (percentages falling short of 100 due to rounding).

Hypothetically, strong mesocyclones should be more common in discrete than nondiscrete supercells, given a lack of inflow disruption, outflow recycling, and merging processes that are more likely to occur with storms embedded in lines and clusters. Since the sample sizes of discrete versus nondiscrete (embedded in clusters and lines) supercell modes are similar, the predominance of various mesocyclone strengths can be compared readily. Weak mesocyclones tended to be slightly more common in nondiscrete TC supercells (67%) compared to discrete (58%), while strong mesocyclones somewhat favored discrete supercell storms (16%) versus nondiscrete supercells (11%).

Compared to nondiscrete midlatitude supercells, TCs contain characteristically high relative humidity boundary layers. For TC supercells, we hypothesized that the resultant lower likelihood of ingestion of adjacent cold outflow (and its attendant weakening of stronger mesocyclones) is offset by the general tendency for weaker buoyancy. However, the validity of that hypothesis cannot be ascertained based solely on the results of this study. In non-TC situations, nondiscrete supercells also carried a slightly higher percentage of weak mesocyclones (34%) than discrete supercells (30%).

Another hypothesis was that TC supercells with strong mesocyclones, and especially discrete supercells, should produce a higher (lower) frequency of strongly

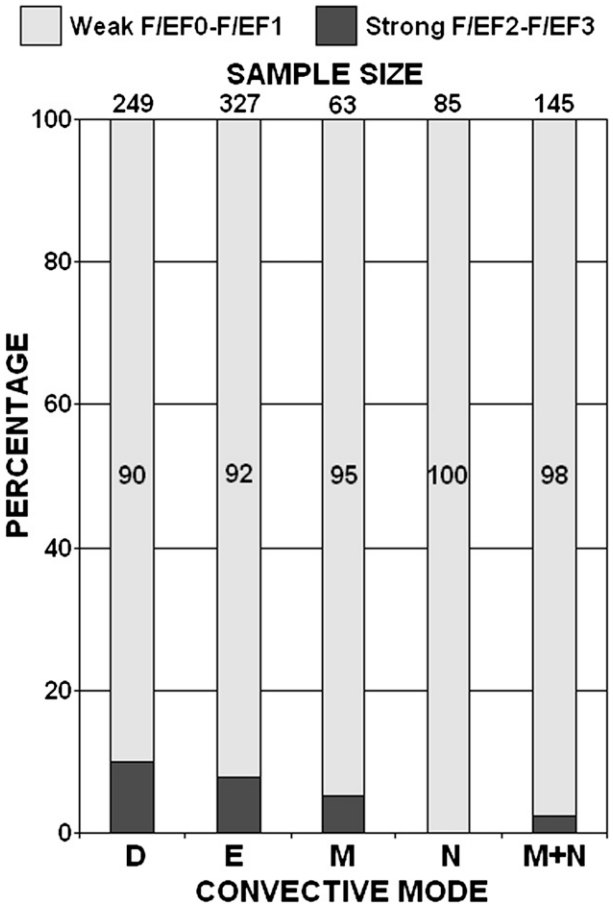

FIG. 5. Percentages of weak and strong tornadoes per mode bin, as labeled: D is discrete supercell, E is embedded supercell (collectively, all supercells in lines plus supercells in clusters), M is marginal (subcriteria) supercell, N is nonsupercell, and M+N combines all modes not meeting supercell criteria. Percentages of weak tornadoes are given in black integers, on bars. Sample size for each mode is given above each bar.

(weakly) rated tornadoes.[8] Only 54 (7%) of all TC tornado events overall were rated strong (EF2 or EF3). Strong tornadoes were far more common with supercells than with marginal or nonsupercells (Fig. 5), and constituted a slightly higher share of tornadoes with discrete versus nondiscrete supercells. No NSTC tornadoes exceeded an EF1 rating. Comparisons of damage ratings with midlatitude, nontropical tornadic supercells (Table 1) indicate that significant (≥EF2) tornadoes are somewhat more common with non-TC supercells, but not as much as the aforementioned difference in mesocyclone strength suggests. This indicates possible influences from the inability of the Weather Surveillance Radar-1988 Doppler (WSR-88D) to resolve mesocyclonic features of the characteristically smaller-scale TC supercells. Sample sizes for damage-rating classes *within* each of the smaller-mode bins (e.g., each form of marginal supercell or of strict nonsupercell) were too small to draw meaningful conclusions.

TABLE 1. Fraction of 2003–11 tornado damage rating occurrence for TCs and non-TC supercells. Numbers may not precisely add to unity due to rounding.

Damage (F/EF category)	TC	Non-TC
≥4	0.00	0.01
3	0.01	0.05
2	0.08	0.12
1	0.33	0.30
0	0.58	0.53

NSTC tornadoes tended not only to yield weaker ratings than their supercellular counterparts, but also to occur closer to TC centers. TCTOR also contains National Hurricane Center ''best track'' data interpolated to the recorded time of each tornadogenesis, followed by derived azimuth and range information (Edwards 2010). Accordingly, 2003–11 TCTOR data were mined for those whole-tornado entries corresponding to strictly nonsupercellular and supercellular modal-event segments herein, yielding polar plots of their distributions with respect to both true north and the estimated TC center at tornado time (Fig. 6). Any entries whose times and locations were corrected for this study, based on radar interrogations, likewise were adjusted in our analysis version of TCTOR prior to computing azimuth and range for Fig. 6. The mean and median radii of NSTC tornadoes from center were 302 and 287 km, respectively, contrasted to the mean and median ranges for supercellular tornadoes of 341 and 342 km. The supercell TC tornado distribution also stretched farther southward, largely because of both discrete and embedded supercells aligned with outer, trailing spiral bands. In general, echo modes with TCs examined for this study tended to show the following characteristics more often with inward extent: ambiguity, unbroken banding (classified here as QLCS), eyewalls or their remnants, and nonconvective to weakly convective rain shields. This accounts for the relative outer distribution of supercellular TC tornadoes. McCaul's (1991)

[8] Damage ratings, especially in the F-scale era, were not necessarily direct functions of actual tornado intensity (Doswell and Burgess 1988), but instead, mere *indicators*, and even then, only if a suitably robust target was hit to represent maximum tornado winds. Given the small, brief nature of TC tornadoes in general, and their occasional spatial juxtaposition with hurricane damage, undersampling issues raised by Doswell and Burgess *may* apply here. No violent (EF4 and EF5) tornadoes were found in the dataset. Further, since maximum EF-scale rating was used as the grid-box filter, the actual ratio of weak (EF0 and EF1) tornadoes to all tornadoes is higher than in the events presented here.

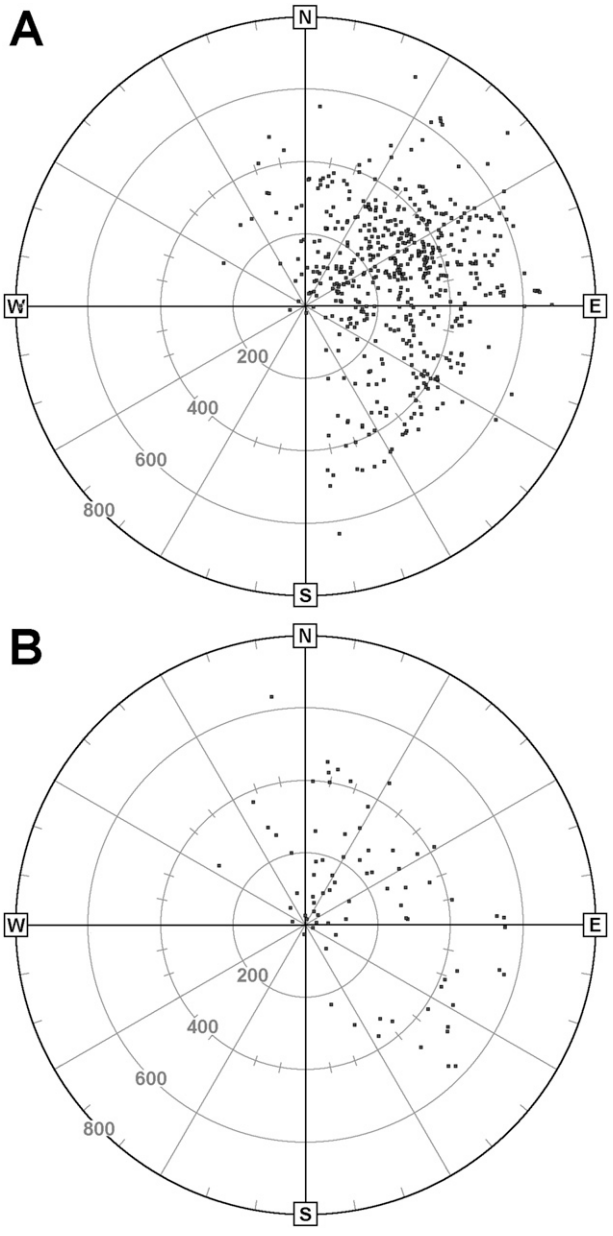

FIG. 6. The TC center-relative plots of 2003–11 TCTOR whole-tornado records (dots) corresponding to modal events classified as (a) fully supercellular and (b) nonsupercellular. Marginal supercells are not plotted. Events appear with respect to north-relative azimuth (tick marks and full radials at 10° and 30° intervals, respectively) and range (km as labeled) from center position, at the time of each tornado. Due to scaling effects, some tornadoes may obscure others in each panel.

sounding-based parameter climatology revealed pronounced weakening of CAPE from the outer rim of the TC inward, as well as of 0–3-km total helicity inside ≈400-km radius. Vertical wind shear tends to decrease inward in most TCs, despite the increase in wind speeds (McCaul 1991; Molinari and Vollaro 2008). Those findings are consistent with the greater proportion of NSTC tornadoes in the inner parts of TCs herein, and the generally weaker storm-relative helicity (SRH) for NSTCs described in section 3d.

d. Environmental results

Using observed soundings, McCaul (1991) showed a juxtaposition of high SRH and at least weak CAPE in TC tornado environments, with buoyancy increasing outward from the center. Additional derived parameters such as most unstable (MU) parcel CAPE,[9] lowest 100-hPa mean mixed layer (ML) CAPE and effective bulk wind difference (EBWD; Thompson et al. 2007) were analyzed in TC tornado environments, along with several other shear-based and kinematic parameters. Most types of environmental data were available for all but four fully supercellular TC tornado events (footnotes 4 and 5), the actual number depending on the parameter(s) being examined. Effective-parcel-based parameters were not available for the 2003–04 TC seasons, accounting for the smaller sample sizes of those analyses.

Parametric distributions for weak (EF0 and EF1) and strong (EF2 and EF3) tornado environments in TCs show some discriminative ability between categories, but with considerable overlap across all variables tested. Figure 7 provides examples for MLCAPE, 0–1-km AGL SRH, 0–6-km AGL bulk wind difference (BWD), and fixed-layer significant tornado parameter (STP; Thompson et al. 2003). Values for the strong tornadoes tended to be somewhat larger for MLCAPE, fixed-layer BWD, and STP, but with considerable overlap. By contrast, the entire 10th–90th percentile range for 0–1-km SRH fit within the same distribution for weak tornadoes. Some compression of the middle 50% of the distributions also was evident in most variables and parameters for strong TC tornadoes; it is unknown if this is a function of actual meteorological distribution or of the sample size being an order of magnitude smaller for strong tornadoes. Similar relative patterns appeared in numerous other parameters, both kinematic and thermodynamic, as well as in bulk indices derived from them such as the SCP (fixed- and effective-layer bases). Such overlap in distributions also may be influenced partly by 1) the considerable spatial overlap between weak and strong tornadoes in the outer envelope of many TCs (where the majority of both classes tends to occur); 2) uncertainty in

[9] All CAPE computations utilized the virtual temperature correction (Doswell and Rasmussen 1994).

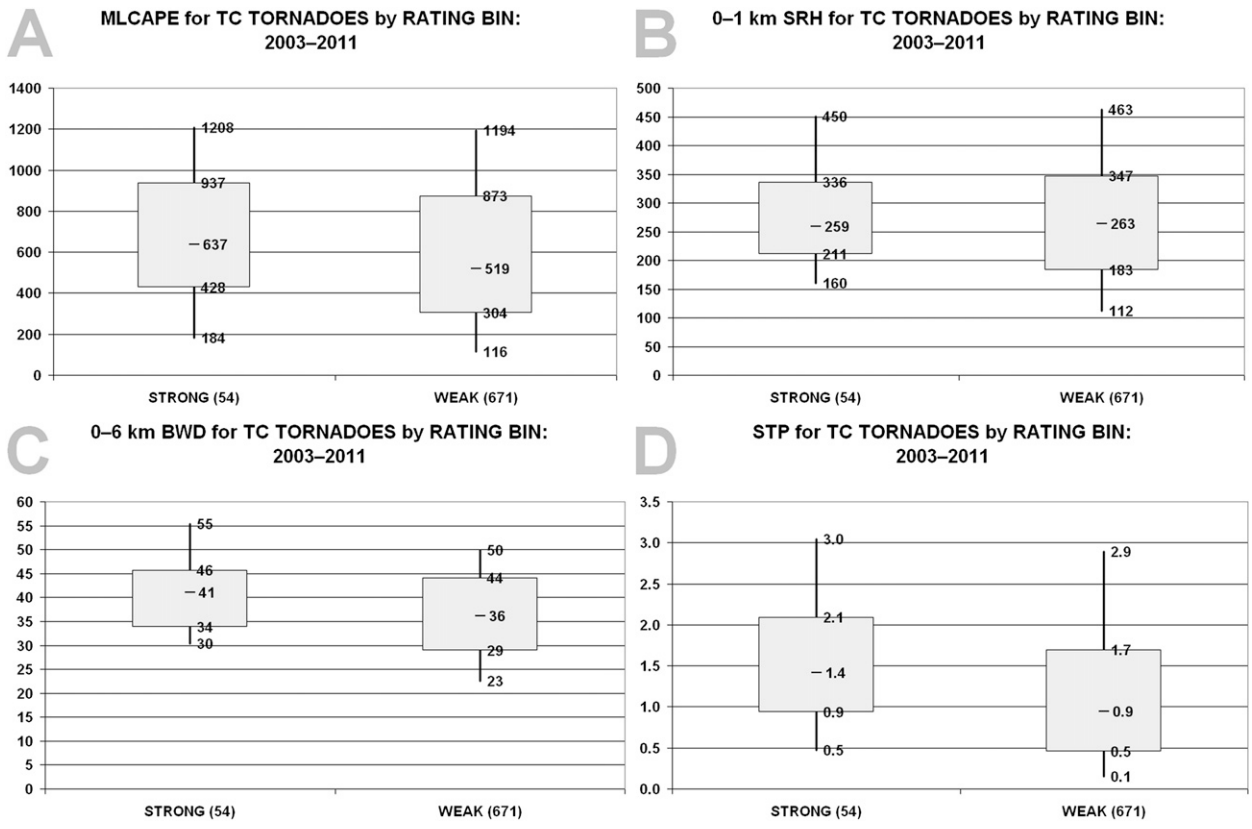

FIG. 7. Box-and-whiskers diagrams, where percentile extents and corresponding values represent 25th–75th for boxes, 10th–90th for whiskers, and 50th at the inbox bar, for (a) MLCAPE (J kg^{-1}), (b) 0–1-km AGL SRH (m^2 s^{-2}), (c) 0–6-km AGL EBWD (kt), and (d) significant tornado parameter (fixed layer). Abscissa labels include sample size in parentheses; ordinate represents parameter magnitude.

damage ratings of ±1 (e.g., Doswell and Burgess 1988); 3) the lack of routinely available observational input above ground level, contributing to the general smoothness of planar fields; and 4) the relatively coarse 40-km grid length of the mesoscale analysis, which should not resolve some kinds of key smaller-scale differences or structures within a TC (e.g., narrow slots of clearing between bands, or baroclinicity related to downdraft-produced θ_e deficits) that can support more robust supercells and tornadoes.

Environmental parameters previously examined for midlatitude, supercellular tornado environments were analyzed for the TC cases, and compared with up to 6897 (depending on environmental data availability) non-TC tornado events from the dataset in Part II that were associated with right-moving supercells. Several of these results are shown in Fig. 8. Similarly to the intensity-category analyses, the smaller sample sizes of the TC subset is associated with compression in the quartile distributions. In general, thermodynamic variables (e.g., Fig. 8a) differentiated the tropical and nontropical tornado environments better than the kinematic ones. Shear-based parameters for TC events did show slightly tighter distributions on the margins (exemplified by 0–1-km SRH in Fig. 3b), but otherwise were similar to their non-TC counterparts. The primary difference between midlatitude and TC tornado situations in this study centers on moisture, as indicated by total precipitable water (PW; Fig. 8c). The 10th percentile of the PW distribution for TCs exceeded the 90th percentile for nontropical tornadoes, with the middle 50% being well separated. This reflects the characteristic thermodynamic environment of TCs, which are very rich in deep-tropospheric moisture. As such, TC supercell environments were decidedly weaker in middle-level lapse rates (e.g., Fig. 8d), which contributed to smaller overall CAPE and a more compressed distribution of the latter (e.g., Fig. 8a). This extended to composite parameters such as SCP and STP (Figs. 8e,f) that substantially incorporate CAPE as part of their formulation.

As in midlatitudes, TC tornadic supercell environments should feature more favorable values of various shear measures than in nonsupercell tornadic convective modes, but with lower values of CAPE (Part II). We

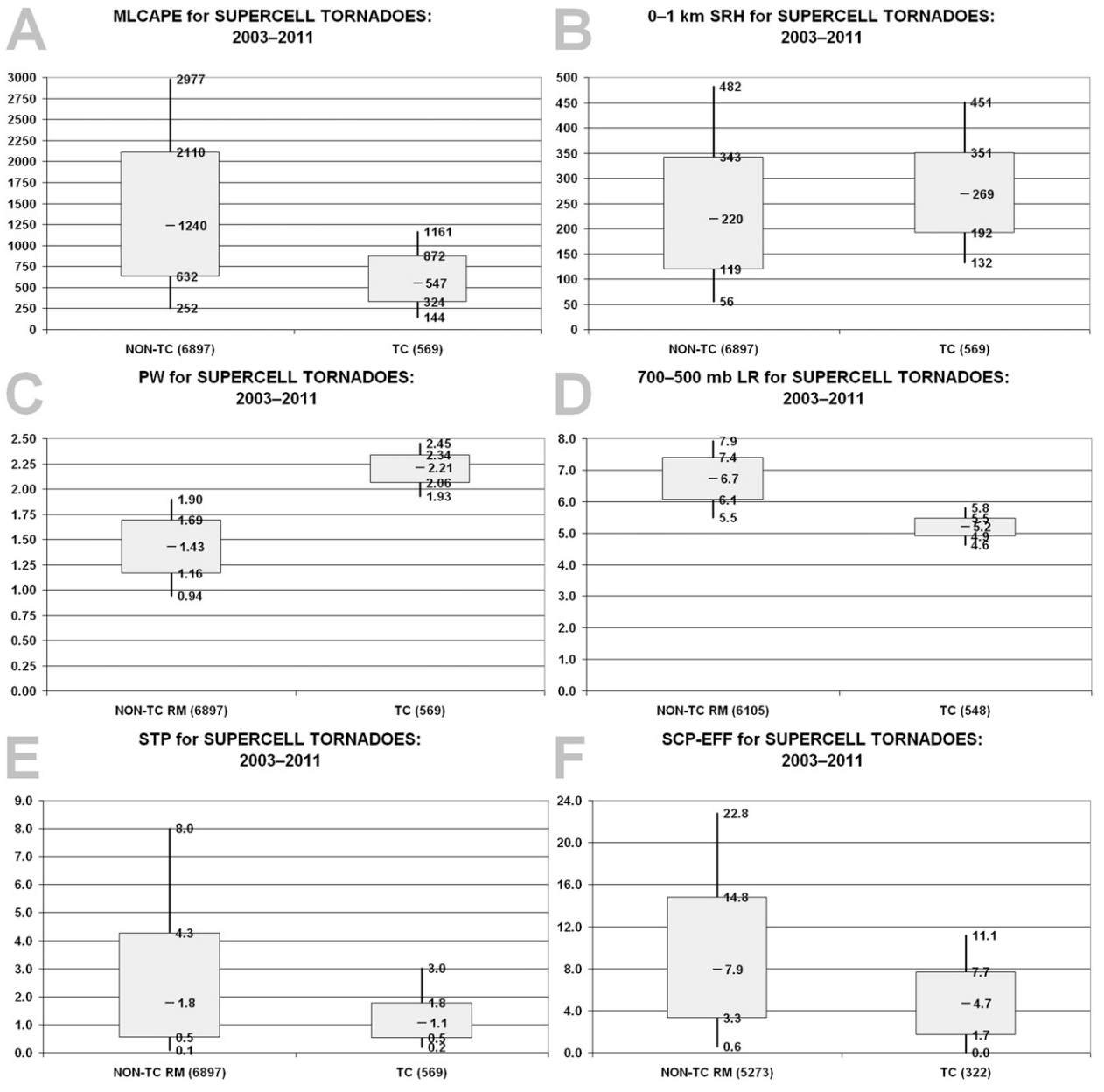

FIG. 8. As in Fig. 7, but for the following parameters in TC and non-TC tornadic supercell datasets: (a) MLCAPE (J kg^{-1}), (b) 0–1-km AGL SRH (m^2 s^{-2}), (c) precipitable water (in.), (d) 700–500-hPa lapse rate (°C km^{-1}), (e) significant tornado parameter (fixed layer), and (f) supercell composite parameter (effective layer).

compared environmental parameters and bulk indices for those two basic categories in order to maximize sample sizes, by including the ''marginal'' storms (those failing to completely meet supercell criteria) with non-supercells in the ''other'' bin. Most kinematic and thermodynamic variables, along with the STP, exhibited little if any meaningful discrimination between supercells and the other modes (e.g., Figs. 9a,b). Exceptions (Figs. 9c,d) were noted in the distributions of the EBWD (Thompson et al. 2007) and, in turn, the effective-layer version of the SCP, given the latter's dependence on EBWD. Relatively high values of BWD and SCP, therefore, may be of some value in diagnosing a potential TC supercell tornado situation, given other favorable features analyzed within the system—namely, the presence of analytically discernible surface boundaries, after Edwards and Pietrycha (2006), and of course the presence of a supercellular convective mode.

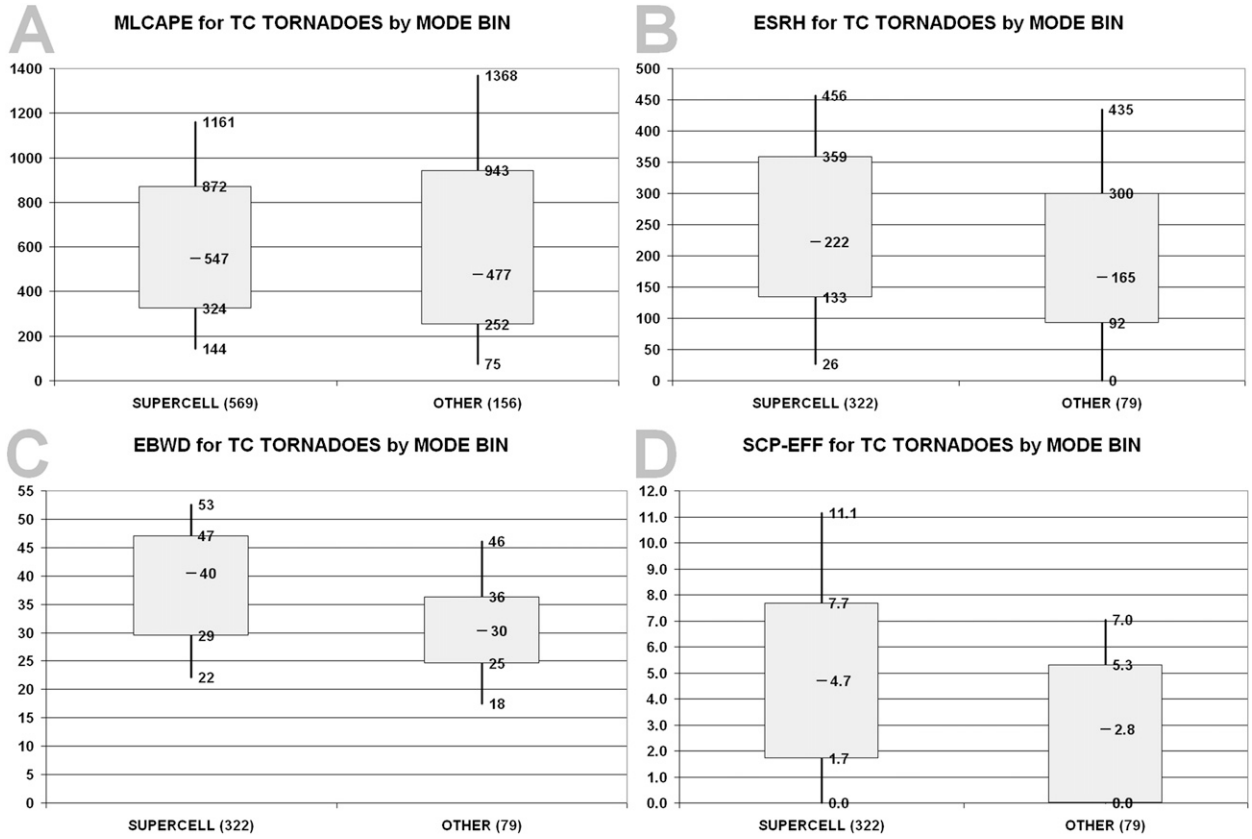

FIG. 9. As in Fig. 7, but for the following parameters in TC supercells and in the remainder of TC tornadic storm modes (''other''): (a) MLCAPE (J kg^{-1}), (b) effective SRH (m^2 s^{-2}), (c) EBWD (kt), and (d) supercell composite parameter (effective layer).

4. Discussion

Examination of associated storm modes indicates that TC tornadoes are far more common with supercells, with a steadily greater potential for stronger (EF1 and EF2) events as convective organization goes from nonsupercell to discrete supercell. However, the resolvable mesoscale environments of strong and weak tornadoes in TCs often are very similar, based on the results of this study. The great relative abundance of moisture in the TC setting, far more so than kinematic measures, seems to account for most of the difference between TC and midlatitude tornado environments.

a. Nonsupercell TC tornadoes

While supercell tornadoes form the bulk of TC tornado events, some TC tornadoes are not spawned by identifiable supercells. Consistently successful diagnosis of foci for NSTC tornadoes, and assessment of changes in tornadic potential of supercells, likely are elusive for this environment, given the currently available gridscales of automated diagnoses.[10] This handicap underscores the need for frequent diagnoses of the TC environment, including careful hand analysis of surface data, to assess the presence and character of subtle baroclinic and kinematic boundaries inside the cyclone envelope (as advocated by Edwards and Pietrycha 2006). Even then, the explicit predictability of NSTC tornadoes, in particular, could stay very poor for a long time, given

- the relatively sparse sample size of documented NSTC tornadoes;
- the apparent similarities in mesoscale environments between TC tornadoes of supercell and nonsupercell origins;

[10] Finer-resolution automated analyses that are out of this study's scope recently have become available as material for similar testing, once TC sample sizes can grow for them, for example, the Space and Time Multiscale Analysis System (STMAS, after Xie et al. 2011) and Real-Time Mesoscale Analysis (RTMA, after De Pondeca et al. 2011). These do not offer as many fields as the SPC mesoanalyses (Bothwell et al. 2002), but can provide base-state variables and (with STMAS) some derived parameters.

- their typically weak and short-lived nature;
- virtually nonexistent direct documentation (i.e., photos, video, mobile radar sampling) of NSTC tornadoes, including supposed eyewall tornadoes, rendering their true frequency highly uncertain;
- lack of high-resolution and proximal radar interrogation in real time to ascertain smaller-scale circulations even than the relatively small TC supercellular mesocyclones; and
- the lack of real-time, finescale observational data that can help forecasters to diagnose, with suitable precision, any small-scale (i.e., 10^{0}–10^{1} km and min in space and time, respectively) patterns of convergence, instability, and vorticity.

At this time, the extent is unknown to which nonsupercell environments are similar to those of midlatitude nonsupercell tornadoes, such as in concentrations of vertical vorticity and convergence (e.g., Caruso and Davies 2005), or if other, altogether different processes are involved.

b. Tornadic and nontornadic environments

In looking at a relatively small sampling of specific events, using observed soundings, Baker et al. (2009) showed that SCP and STP could be used to distinguish tornadic from nontornadic environments in one particular TC, Ivan of 2004. By contrast, null events were outside the scope of this study; therefore, we did not collect nontornadic supercell events that could be used to test their null-event results on gridded analyses, and in TCs other than Ivan. The comparison of nontornadic supercell environments with those of tornadic storms, across multiple TCs, is an area that may be worth further exploration, especially if null and tornadic supercells, in particular, do not exhibit much spatial overlap at these environmental-analysis grid scales.

As noted in section 1, prior studies have found important influences of poorly resolved, small-scale processes on TC tornado potential. Clearly, considerable further study is needed for better documentation of the near-storm tornado environment in TCs, both supercellular and nonsupercellular, for better differentiation of tornadic versus nontornadic regimes by the forecaster. Given the gridscales employed herein, near-storm-scale processes, such as in situ cold pool generation, likely will not be known in an operational setting—one possible, eventual exception being dropsonde deployments (as studied by Bogner et al. 2000 and Baker et al. 2009) into such regimes that, in turn, reach the forecaster in near–real time. Careful diagnosis and conceptual modeling of the TC tornado environment remains necessary for forecasters—for example, evaluating the relative position of an embedded storm to that of its broader band or cluster, for assessing its potential interaction with small-scale baroclinic boundaries generated from within the cluster or band. One such area of acute, diagnostic scrutiny in the operational setting may be along the inner rim of a spiral band, where Powell (1990) noted relative maxima in cyclonic vorticity and convergence.

Within the framework of numerical guidance and research, some of these issues may be investigated through higher-resolution TC modeling. Future plans for the Hurricane Weather Research and Forecasting model (HWRF) include 3-km and/or 1-km moving inner nests (Zhang et al. 2010), which conceivably could resolve some tornadic storms and their immediate environments within the TC envelope. With such modeling on the way, assessment of its capabilities to diagnose both supercell and nonsupercell tornado regimes in TCs should be performed.

Acknowledgments. The SPC Science Support Branch made various forms of data available. Greg Carbin (SPC) provided the base tornado data used to construct TCTOR. Steve Weiss (SPC) offered very helpful internal review and suggestions. GRLevelX software was used to interrogate archived level-2 and -3 radar data for convective-mode analyses.

REFERENCES

Agee, E. M., and A. Hendricks, 2011: An assessment of the climatology of Florida hurricane-induced tornadoes (HITs): Technology versus meteorology. *J. Climate,* **24,** 5218–5222.

Andra, D. L., Jr., 1997: The origin and evolution of the WSR-88D mesocyclone recognition nomogram. Preprints, *28th Conf. on Radar Meteorology,* Austin, TX, Amer. Meteor. Soc., 364–365.

Baker, A. K., M. D. Parker, and M. D. Eastin, 2009: Environmental ingredients for supercells and tornadoes within Hurricane Ivan. *Wea. Forecasting,* **24,** 223–243.

Barnes, G. M., E. J. Zipser, D. Jorgensen, and F. Marks Jr., 1983: Mesoscale and convective structure of a hurricane rainband. *J. Atmos. Sci.,* **40,** 2125–2137.

Benjamin, S. G., and Coauthors, 2004: An hourly assimilation–forecast cycle: The RUC. *Mon. Wea. Rev.,* **132,** 495–518.

——, and Coauthors, 2007: From radar-enhanced RUC to the WRF-based Rapid Refresh. Preprints, *18th Conf. on Numerical Weather Prediction,* Park City, UT, Amer. Meteor. Soc., J3.4. [Available online at http://ams.confex.com/ams/pdfpapers/124827.pdf.]

Bogner, P. B., G. M. Barnes, and J. L. Franklin, 2000: Conditional instability and shear for six hurricanes over the Atlantic Ocean. *Wea. Forecasting,* **15,** 192–207.

Bothwell, P. D., J. A. Hart, and R. L. Thompson, 2002: An integrated three-dimensional objective analysis scheme in use at the Storm Prediction Center. Preprints, *21st Conf. on Severe Local Storms,* San Antonio, TX, Amer. Meteor. Soc., JP3.1. [Available online at https://ams.confex.com/ams/SLS_WAF_NWP/techprogram/paper_47482.htm.]

Caruso, J. M., and J. M. Davies, 2005: Tornadoes in non-mesocyclone environments with pre-existing vertical vorticity along convergence boundaries. *Electron. J. Oper. Meteor.,* **6** (4), 1–36. [Available online at http://www.nwas.org/ej/pdf/2005-EJ4.pdf.]

Cione, J. J., P. G. Black, and S. H. Houston, 2000: Surface observations in the hurricane environment. *Mon. Wea. Rev.,* **128,** 1550–1561.

Curtis, L., 2004: Midlevel dry intrusions as a factor in tornado outbreaks associated with landfalling tropical cyclones from the Atlantic and Gulf of Mexico. *Wea. Forecasting,* **19,** 411–427.

De Pondeca, M. S. F. V., and Coauthors, 2011: The real-time mesoscale analysis at NOAA's National Centers for Environmental Prediction: Current status and development. *Wea. Forecasting,* **26,** 593–612.

Doswell, C. A., III, 1987: The distinction between large-scale and mesoscale contribution to severe convection: A case study example. *Wea. Forecasting,* **2,** 3–16.

——, and D. W. Burgess, 1988: On some issues of United States tornado climatology. *Mon. Wea. Rev.,* **116,** 495–501.

——, and E. N. Rasmussen, 1994: The effect of neglecting the virtual temperature correction on CAPE calculations. *Wea. Forecasting,* **9,** 625–629.

Edwards, R., 2003: Rating tornado damage: An exercise in subjectivity. Preprints, *First Symp. on F-Scale and Severe-Weather Damage Assessment,* Long Beach, CA, Amer. Meteor. Soc., P1.2. [Available online at https://ams.confex.com/ams/annual2003/techprogram/paper_55307.htm.]

——, 2010: Tropical cyclone tornado records for the modernized NWS era. Preprints, *25th Conf. on Severe Local Storms,* Denver, CO, Amer. Meteor. Soc., P3.1. [Available online at http://ams.confex.com/ams/pdfpapers/175269.htm.]

——, 2012: Tropical cyclone tornadoes: A review of knowledge in research and prediction. *Electron. J. Severe Storms Meteor.,* **7** (6), 1–61. [Available online at http://www.ejssm.org/ojs/index.php/ejssm/article/view/97/84.]

——, and A. E. Pietrycha, 2006: Archetypes for surface baroclinic boundaries influencing tropical cyclone tornado occurrence. Preprints, *23rd Conf. on Severe Local Storms,* Saint Louis, MO, Amer. Meteor. Soc., P8.2. [Available online at http://ams.confex.com/ams/pdfpapers/114992.pdf.]

Fujita, T. T., 1993: Damage survey of Hurricane Andrew in south Florida. *Storm Data,* Vol. 34, No. 8, 25–29. [Available from National Climatic Data Center, Asheville, NC 28801.]

McCaul, E. W., Jr., 1987: Observations of the Hurricane ''Danny'' tornado outbreak of 16 August 1985. *Mon. Wea. Rev.,* **115,** 1206–1223.

——, 1991: Buoyancy and shear characteristics of hurricane–tornado environments. *Mon. Wea. Rev.,* **119,** 1954–1978.

——, and M. L. Weisman, 1996: Simulations of shallow supercell storms in landfalling hurricane environments. *Mon. Wea. Rev.,* **124,** 408–429.

——, D. E. Buechler, S. J. Goodman, and M. Cammarta, 2004: Doppler radar and lightning network observations of a severe outbreak of tropical cyclone tornadoes. *Mon. Wea. Rev.,* **132,** 1747–1763.

McNulty, R. P., 1978: On upper tropospheric kinematics and severe weather occurrence. *Mon. Wea. Rev.,* **106,** 662–672.

——, 1985: A conceptual approach to thunderstorm forecasting. *Natl. Wea. Dig.,* **10** (2), 26–30.

Molinari, J., and D. Vollaro, 2008: Extreme helicity and intense convective towers in Hurricane Bonnie. *Mon. Wea. Rev.,* **136,** 4355–4372.

Morin, M. J., M. D. Parker, K. A. Hill, and G. M. Lackmann, 2010: A numerical investigation of supercells in landfalling tropical cyclones. Preprints, *25th Conf. on Severe Local Storms,* Denver, CO, Amer. Meteor. Soc., P3.3. [Available online at http://ams.confex.com/ams/pdfpapers/175965.pdf.]

Novlan, D. J., and W. M. Gray, 1974: Hurricane-spawned tornadoes. *Mon. Wea. Rev.,* **102,** 476–488.

Orton, R., 1970: Tornadoes associated with Hurricane Beulah on September 19–23, 1967. *Mon. Wea. Rev.,* **98,** 541–547.

Powell, M. D., 1990: Boundary layer structure and dynamics in outer hurricane rainbands. Part I: Mesoscale rainfall and kinematic structure. *Mon. Wea. Rev.,* **118,** 891–917.

Rao, G. V., J. W. Scheck, R. Edwards, and J. T. Schaefer, 2005: Structures of mesocirculations producing tornadoes associated with Tropical Cyclone Frances (1998). *Pure Appl. Geophys.,* **162,** 1627–1641.

Schneider, R. S., and A. R. Dean, 2008: A comprehensive 5-year severe storm environment climatology for the continental United States. Preprints, *24th Conf. on Severe Local Storms,* Savannah, GA, Amer. Meteor. Soc., 16A.4. [Available online at http://ams.confex.com/ams/pdfpapers/141748.pdf.]

Schultz, L. A., and D. J. Cecil, 2009: Tropical cyclone tornadoes, 1950–2007. *Mon. Wea. Rev.,* **137,** 3471–3484.

Smith, B. T., R. L. Thompson, J. S. Grams, C. Broyles, and H. E. Brooks, 2012: Convective modes for significant severe thunderstorms in the contiguous United States. Part I: Storm classification and climatology. *Wea. Forecasting,* **27,** 1114–1135.

Spratt, S. M., D. W. Sharp, P. Welsh, A. Sandrik, F. Alsheimer, and C. Paxton, 1997: A WSR-88D assessment of tropical cyclone outer rainband tornadoes. *Wea. Forecasting,* **12,** 479–501.

Stumpf, G. J., A. Witt, E. D. Mitchell, P. L. Spencer, J. T. Johnson, M. D. Eilts, K. W. Thomas, and D. W. Burgess, 1998: The National Severe Storms Laboratory mesocyclone detection algorithm for the WSR-88D. *Wea. Forecasting,* **13,** 304–326.

Thompson, R. L., R. Edwards, J. A. Hart, K. L. Elmore, and P. Markowski, 2003: Close proximity soundings within supercell environments obtained from the Rapid Update Cycle. *Wea. Forecasting,* **18,** 1243–1261.

——, C. M. Mead, and R. Edwards, 2007: Effective storm-relative helicity and bulk shear in supercell thunderstorm environments. *Wea. Forecasting,* **22,** 102–115.

——, B. T. Smith, J. S. Grams, A. R. Dean, and C. Broyles, 2012: Convective modes for significant severe thunderstorms in the contiguous United States. Part II: Supercell and QLCS tornado environments. *Wea. Forecasting,* **27,** 1136–1154.

Wakimoto, R. M., and J. W. Wilson, 1989: Non-supercell tornadoes. *Mon. Wea. Rev.,* **117,** 1113–1140.

WSEC, 2006: A recommendation for an enhanced Fujita scale (EF-scale). Wind Science and Engineering Center, Texas Tech University, 95 pp. [Available online at http://www.spc.noaa.gov/faq/tornado/ef-ttu.pdf.]

Xie, Y., S. Koch, J. McGinley, S. Albers, P. E. Bieringer, M. Wolfson, and M. Chan, 2011: A space–time multiscale analysis system: A sequential variational analysis approach. *Mon. Wea. Rev.,* **139,** 1224–1240.

Zhang, Z., S. G. Gopalakrishnan, K. Yeh, R. F. Rogers, S. D. Aberson, F. D. Marks, and T. Quirino, 2010: The HWRFx modeling system: The high resolution hurricane forecast test. Preprints, *29th Conf. on Hurricanes and Tropical Meteorology,* Tucson, AZ, Amer. Meteor. Soc., 3C.3. [Available online at http://ams.confex.com/ams/pdfpapers/168948.pdf.]